ELSEVIER

Journal of Alloys and Compounds 230 (1995) 35–41

Journal of ALLOYS AND COMPOUNDS

Magnetic properties of $UFe_{10}Si_2$ single crystal

P. Estrela[a], M. Godinho[a], A.P. Gonçalves[b], M. Almeida[b], J.C. Spirlet[c]

[a]*Departamento de Física, Faculdade de Ciências da Universidade de Lisboa, Campo Grande, Ed. C1, P-1700 Lisboa, Portugal*
[b]*Departamento de Química, Instituto Tecnológico e Nuclear, P-2686 Sacavém Codex, Portugal*
[c]*European Commission, Joint Research Centre, Institute of Transuranium Elements, Postfach 2340, D-76125 Karlsruhe, Germany*

Received 8 May 1995

Abstract

$UFe_{10}Si_2$ single crystals with $ThMn_{12}$-type structure were studied by X-ray diffraction and magnetisation measurements. A uniaxial anisotropy, a saturation magnetisation of 19.5 μ_B f.u.$^{-1}$ and a type-1 first order magnetisation process, for fields applied along the hard *a* axis, were observed in agreement with previous powder results. The anisotropy constants K_1, K_2 and K_3 were obtained from the magnetisation curves along the hard axis. The analysis of the first order magnetisation process, through the simultaneous measurement of the longitudinal ($\parallel H$) and transverse ($\perp H$) components of the magnetisation, assigned it to a rotation of the total magnetisation. The results indicate an important contribution of the uranium sublattice to the magnetism in this compound.

Keywords: $UFe_{10}Si_2$; Single crystal; Magnetic properties; Crystal structure

1. Introduction

The $UFe_{10}Si_2$ compound, first reported in 1989 [1,2], has attracted considerable interest due to its large uniaxial magnetic anisotropy, saturation magnetisation (approximately 19 μ_B f.u.$^{-1}$) and Curie temperature (650 K) [3–10]. The nonexistence of single crystals has limited the characterisation of this compound and all previous measurements have been performed on polycrystalline, and in some cases even polyphasic, samples. The role of the U atoms in the magnetic properties remained unclear.

$UFe_{10}Si_2$ crystallises in the tetragonal $ThMn_{12}$-type structure (space group *I4/mmm*) where the uranium atoms occupy the 2a sites, the silicon atoms are randomly located in the 8f and 8j sites, and the 8i sites are occupied only by iron [5]. The magnetic anisotropy of this compound, as in other $AFe_{12-x}M_x$ systems (A = actinide, lanthanide or Y) with this type of structure, is a consequence of the tetragonal symmetry. The large saturation magnetisation is due to the large number of Fe atoms completely occupying the 8i positions.

The magnetic state of the uranium sublattice in $UFe_{10}Si_2$ has been discussed by Andreev and coworkers [6,7] suggesting a small uranium magnetic moment due to a cancelation of two large orbital and spin contributions, as proposed for UFe_2 [11]. The large magnetic anisotropy and the existence of a field induced magnetic process were considered as an indication of a considerable contribution of the uranium sublattice to the magnetisation in $UFe_{10}Si_2$.

Recently we have been able to grow large single crystals of $UFe_{10}Si_2$ [8]. In this work we report the first magnetisation measurements on single crystals.

2. Experimental details

Samples with $UFe_{9.2}Si_{1.8}$ nominal composition were prepared from the induction melting of the elements (99.9% purity or better) in a levitation cold crucible under vacuum. These samples were used as bulk charges for the crystal growth of large single crystals using the Czochralski method as described previously [8]. The density of the bulk charges, as well of the pulled material, was measured by the pyknometer method.

A small single crystal ($0.090 \times 0.082 \times 0.054$ mm^3) was isolated from the bulk polycrystalline material and glued on the top of a glass fibre. This fibre was transferred to a goniometer head mounted on an

SSDI 0925-8388(95)01938-3

Enraf–Nonius CAD-4 diffractometer with a graphite monochromatised Mo Kα radiation ($\lambda = 0.71073$ Å). The least squares refinement of the 2θ values of 25 reflections from various regions of the reciprocal space in the range $17° \leq 2\theta \leq 40°$ was used to obtain the unit cell parameters.

The data set was collected at room temperature in an ω-2θ scan mode ($\Delta\omega = 0.80 + 0.35 \tan\theta$). Five reflections were monitored as orientation and three as intensity standards at 4 h intervals during the data collection; no variation larger than 3% was observed. The intensities of the 2103 measured reflections (with $2\theta < 80°$) were corrected for absorption according to North et al. [12] and for polarisation and Lorentz effects. The equivalent reflections were averaged, resulting in 336 unique reflections from which 313 with $I \geq 3\sigma(I)$ were considered significant.

The structure was refined using the UPALS program [13]. Scattering factors for neutral atoms as well as anomalous dispersion corrections were taken from Ref. [14]. A type-1 isotropic secondary extinction correction, according to the Becker and Coppens formalism [15,16] was refined together with a scale factor, two position parameters (x for 8j and 8i positions), three occupation factors and four isotropic temperature factors. The occupation by Fe and Si atoms of the 8f, 8j and 8i crystallographic positions was constrained to vary within the full site occupancy. The least squares procedure converged to $R = \sum|F_{obs} - F_{calc}|/\sum|F_{obs}| = 0.03848$ and $Rw = 0.03841$ ($w = 1/\sigma^2$) final values with the 8i position only occupied by iron atoms and the silicon partially occupying the 8f and 8j positions. Crystal data and experimental details of the structure determination are presented in Table 1. Atomic positions, occupation factors and thermal displacement parameters are compiled in Table 2.

Magnetisation measurements were performed on a crystal with approximated dimensions $2.3 \times 1.1 \times 1.0$ mm^3 using a SQUID magnetometer which allows the simultaneous determination of the longitudinal ($M \| H$) and transverse ($M \perp H$) components of the total magnetisation. The measurements were performed for temperatures between 5 and 250 K and for magnetic fields in the range −5.5 to 5.5 T.

3. Results and discussion

Observed values for density of the pulled single crystal and polycrystalline bulk material cleaned from surface oxides were 8.54(5) and 8.41(8) g cm^{-3} respectively. These values are much closer to the calculated density for $UFe_{10}Si_2$ (8.54 g cm^{-3}) than for $UFe_{9.2}Si_{1.8}$ (8.04 g cm^{-3}), indicating that the bulk and the pulled material have no vacancy, which is at variance with prior suppositions [8]. The observed existence of a

Table 1
Crystal data and details of $UFe_{10}Si_2$ structure determination

Chemical formula	$UFe_{10}Si_2$
Formula weight (g mol^{-1})	852.67
Crystal system	Tetragonal
Space group [17]	*I4/mmm* (No. 139)
a (Å)	8.3729(5)
c (Å)	4.7269(4)
V (Å^3)	331.381(37)
Z	2
D_{calc} (g cm^{-3})	8.54
μ(Mo Kα) (cm^2 g^{-1})	52.13
Approximate crystal dimensions (mm^3)	$0.09 \times 0.08 \times 0.05$
Radiation, wavelength (Å)	Mo Kα, 0.71073
Monochromator	Graphite
Temperature (K)	295
θ range (deg)	1.5–37
ω-2θ scan	$\Delta\omega = 0.80 + 0.35 \tan\theta$
Data set	$-15 \leq h \leq 15$; $-15 \leq k \leq 15$; $-8 \leq l \leq 8$
Crystal-to-receiving-aperature distance (mm)	173
Horizontal, vertical aperture (mm)	4, 4
Total data	2103
Unique data	336
Observed data ($I \geq 3\sigma(I)$)	313
Number of refined parameters	11
Final agreement factors[a]	
$R = \Sigma\|F_{obs} - F_{calc}\|/\Sigma\|F_{obs}\|$	0.03848
$wR = \{\Sigma[w(\|F_{obs}\| - \|F_{calc}\|)^2]/w\|F_{obs}\|^2\}^{1/2}$	0.03841
$S = [\Sigma w(\|F_{obs}\| - \|F_{calc}\|^2/(m-n)]^{1/2}$	1.062

[a] m, number of observations; n, number of variables.

Table 2
Atomic positions (x, y, z), occupation factors (O.F.) and temperature factors (U) obtained in the refinement. The temperature factor is expressed as $T(\theta) = \exp[-8\pi^2 U(\sin\theta/\lambda)^2]$

Atom	Position	x	y	z	O.F.	$U \times 10^2$ (Å^2)
U	2a	0	0	0	1	0.43(2)
Fe	8f	1/4	1/4	1/4	0.56(2)	0.31(3)
Si	8f	1/4	1/4	1/4	0.44(2)	0.31(3)
Fe	8j	0.2815(2)	1/2	0	0.83(3)	0.56(3)
Si	8j	0.2815(2)	1/2	0	0.17(3)	0.56(3)
Fe	8i	0.3563(2)	0	0	1.01(3)	0.54(3)
Si	8i	0.3563(2)	0	0	−0.01(3)	0.54(3)

considerable amount of surface oxides in the bulk charges is consistent with the idea of some uranium oxidation and with the formation of a poor uranium material compared with the nominal composition. The uranium consumption by oxidation compensates the Fe–Si deficiency explaining why this nominal composition was required to obtain a congruent melting $UFe_{10}Si_2$ sample (the 9.2:1.8 and the 10:2 iron–silicon relations are identical).

The refinement of X-ray diffraction data is not sensitive enough to differentiate between the existence of a vacancy and small changes in the (Fe–Si) concentration. However it confirms previous X-ray powder diffraction results indicating the $ThMn_{12}$-type structure in this compound [1]. Considering a full occupancy of all positions, the structural refinement shows that the silicon atoms are located in the 8f and 8j positions in agreement with Rietveld refinements performed on X-ray powder diffraction patterns [5]. This also agrees with previous results on lanthanide isostructural compounds showing that, probably due to enthalpy effects, the silicon atoms share the 8f and 8j positions with the iron atoms [18]. Interatomic distances and average number of nearest neighbours for the different crystallographic positions are listed in Table 3.

The magnetisation curves $M(H)$ at different temperatures with the c axis respectively parallel and perpendicular to the applied magnetic field are shown in Fig. 1. The easy direction magnetisation curves

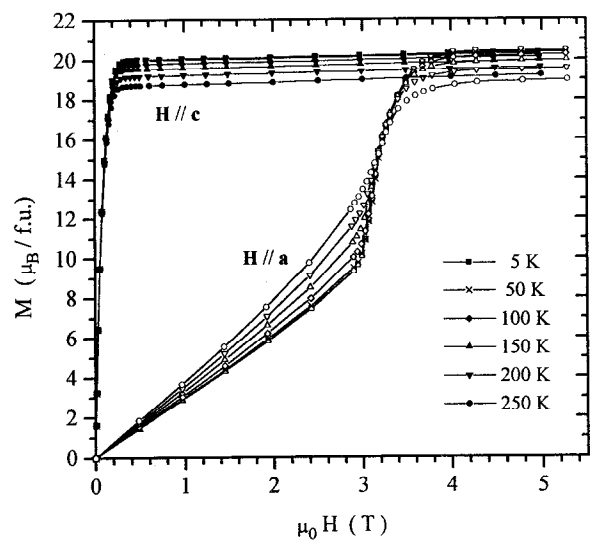

Fig. 1. Field dependence of the $UFe_{10}Si_2$ magnetisation for the easy ($H\|c$—full symbols) and hard ($H\perp c$—open symbols) directions for different temperatures. The curves have been corrected for the demagnetising field.

($H\|c$) show a typical ferromagnetic behaviour, reaching saturation at relatively low fields (0.2 T $\leq \mu_0 H \leq$ 0.3 T), while the hard direction magnetisation curves show a type-1 first order magnetisation process (FOMP), as first reported by Andreev et al. [6] from magnetic measurements on aligned powder samples. In both the easy and hard magnetisation directions no hysteresis was observed. Transverse magnetisation

Table 3
$UFe_{10}Si_2$ interatomic distances (d) and nearest neighbours (NN) average numbers

	NN	Atoms	d (Å)		NN	Atoms	d (Å)
U(2a)	8	(Fe, Si)(8f)	3.187	(Fe, Si)(8f)	2	(Fe, Si)(8f)	2.363
	8	(Fe, Si)(8j)	2.989		4	(Fe, Si)(8j)	2.418
	4	Fe(8i)	2.983		4	Fe(8i)	2.563
					2	U(2a)	3.187
(Fe, Si)(8j)	4	(Fe, Si)(8f)	2.418	Fe(8i)	4	(Fe, Si)(8f)	2.563
	2	(Fe, Si)(8j)	2.587		2	(Fe, Si)(8j)	2.646
	2	Fe(8i)	2.646		2	(Fe, Si)(8j)	2.630
	2	Fe(8i)	2.630		1	Fe(8i)	2.406
	2	U(2a)	2.989		4	Fe(8i)	2.912
					1	U(2a)	2.983

measurements with the magnetic field applied along the easy c axis clearly show an isotropic (a,b) plane. This isotropy was confirmed by the longitudinal magnetisation measurements obtained with the magnetic field applied along the [100], [010] and [110]; these show identical magnetisation curves.

The magnetisation curves along the easy axis c show a small slope after approaching saturation which is the same as for the hard magnetisation curve after the FOMP. The saturation magnetisation M_S, obtained from the extrapolation of the easy direction magnetisation curve to $H = 0$, decreases with increasing temperature (19.5 μ_B f.u.$^{-1}$ and 17.8 μ_B f.u.$^{-1}$ at $T = 5$ and 250 K respectively). The measured magnetisation values at 5.5 T are similar for both the easy and hard magnetisation directions.

Our value of $M_S = 19.5$ μ_B f.u.$^{-1}$ at 5 K is higher than 16.4 μ_B f.u.$^{-1}$ reported for oriented polycrystals [6,9]. Isostructural $RFe_{10}Si_2$ compounds with nonmagnetic R = Y or Lu present comparable values: a saturation magnetisation of 19.0 μ_B f.u.$^{-1}$ [19], 18.2 μ_B f.u.$^{-1}$ [20] at 1.5 K and 18.0 μ_B f.u.$^{-1}$ at 4.5 K [6] was derived from magnetisation measurements on free or aligned $YFe_{10}Si_2$ powder samples. In the same type of measurements the lutetium compound presents a saturation magnetisation of 18.3 μ_B f.u.$^{-1}$ at 1.5 K [20] and 17.7 μ_B f.u.$^{-1}$ at 4.5 K [21]. These values are in good agreement with those derived from ^{57}Fe Mössbauer spectroscopy, assuming a conversion factor of 14.5 T μ_B^{-1} [22], which gives 18.5 μ_B f.u.$^{-1}$ at 14 K [7] and 18.0 μ_B f.u.$^{-1}$ at 77 K [23] for the yttrium and lutetium compounds respectively. However, a comparison with neutron diffraction data on the $YFe_{10}Si_2$, that shows a total magnetic moment of 21.1 μ_B f.u.$^{-1}$ [19], reveals an incomplete alignment of the crystals with the field. Assuming a negligible small contribution from the conduction electrons, a conversion factor of 12.7 T μ_B^{-1} for these types of compound can be deduced. Using this value and taking from Ref. [7] an average hyperfine field of 23 T per Fe for the iron atoms in $UFe_{10}Si_2$, a contribution of the iron sublattice for the saturation magnetisation of 18.1 μ_B f.u.$^{-1}$ can also be deduced. Comparing this value with the single crystal saturation magnetisation (19.5 μ_B f.u.$^{-1}$), a ferromagnetic interaction between the uranium and iron sublattices is suggested with a uranium magnetic moment of 1.4 μ_B. This value is significantly higher than the $\mu_U = 0.5$ μ_B reported previously [7] and shows a significant difference between the spin and orbital moments of uranium.

The longitudinal M_a and transverse M_c magnetisation curves in the $H \| a$ configuration are presented in Fig. 2. We notice that the two magnetisation components increase with the applied field up to the type-1 FOMP. This result can be explained by assuming a small misalignment of the a axis relative to the applied

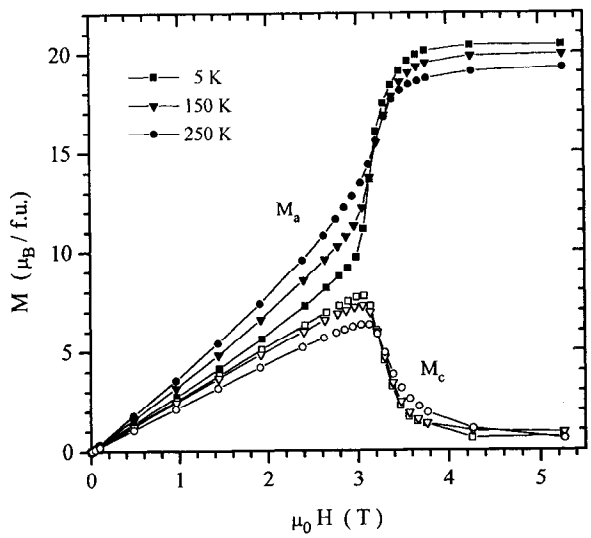

Fig. 2. Longitudinal (full symbols) and transverse (open symbols) magnetisation curves for $H \perp c$ in $UFe_{10}Si_2$. The curves have been corrected for the demagnetising field.

magnetic field. At zero field the domains are randomly oriented along the easy direction of magnetisation (c_+ and c_-), giving two identical symmetrical contributions to the total magnetisation, M_+ and M_-. If there is a small misalignment of the crystal, the two directions c_+ and c_- are no longer equivalent in the field direction. Considering a smaller angle between c_+ and the applied field, by increasing the magnetic field some domains initially oriented along c_- will change their orientations to c_+, showing a nonzero transverse magnetisation value. At the same time both M_+ and M_- will slowly rotate towards the magnetic field direction. The conjugation of these two mechanisms leads to an increase with applied field of both the longitudinal and the transverse components of the total magnetisation vector. When the energy corresponding to an orientation of the domains along the applied field is stronger than the anisotropy energy, the FOMP occurs due to a rotation of the magnetisation vector to the field direction. This rotation is detected as a jump on the magnetisation curve with the longitudinal component increasing rapidly to the saturation value and the transverse component decreasing to zero. This process is observed in the whole temperature range studied. For reverse magnetic field the magnetisation curves (longitudinal and transverse) show exactly the same behaviour as for positive fields, with negative values for both components of the magnetisation vector, confirming the above explanation.

The anisotropy field H_A given by the field at which the extrapolation of the initial part ($\mu_0 H < 2.5$ T) of the hard direction magnetisation curve intercepts the easy direction curve has the value 7.1 T at $T = 5$ K.

With this definition, the anisotropy constant K_1 is simply given by $K_1 = H_A M_S/2$.

The magnetisation curve for a uniaxial crystal with the magnetic field applied perpendicular to the symmetry axis is given by [24]

$$HM_S = 2K_1\frac{M}{M_S} + 4K_2\left(\frac{M}{M_S}\right)^3 + 6K_3\left(\frac{M}{M_S}\right)^5$$

From the hard magnetisation curve the values of the anisotropy constants K_2 and K_3 were obtained (Fig. 3). At $T = 5$ K for $M_S = 19.5\ \mu_B$ f.u.$^{-1}$ the anisotropy constant values are $K_1 = 38.5 \times 10^6$ erg cm^{-3}, $K_2 = -16.1 \times 10^6$ erg cm^{-3} and $K_3 = 3.9 \times 10^6$ erg cm^{-3}.

These values for the anisotropy constants fall in the range required for the occurrence of a type-1 FOMP occurring with the magnetic field applied perpendicular to the magnetisation symmetry axis [24]. The field at which the FOMP occurs is almost temperature independent ($H_C = 3.13$ T at 5 K and $H_C = 3.22$ T at 250 K). This small temperature dependence was also observed for oriented powder samples [9] where an almost constant value of 3.2 T was obtained for temperatures up to 300 K.

Since the origin of the observed FOMP is simply a rotation of the magnetisation vector resulting from an energy balance, considering that the total energy is the same in the two phases, the critical magnetisation M_C and the critical magnetic field H_C at which the FOMP should occur can be calculated by a simple analysis of the anisotropy constants. The calculated values of the critical magnetisation M_C^{calc} and field H_C^{calc} are plotted in Figs. 4 and 5 respectively. M_C^{calc} increases with temperature in the same way as the observed values,

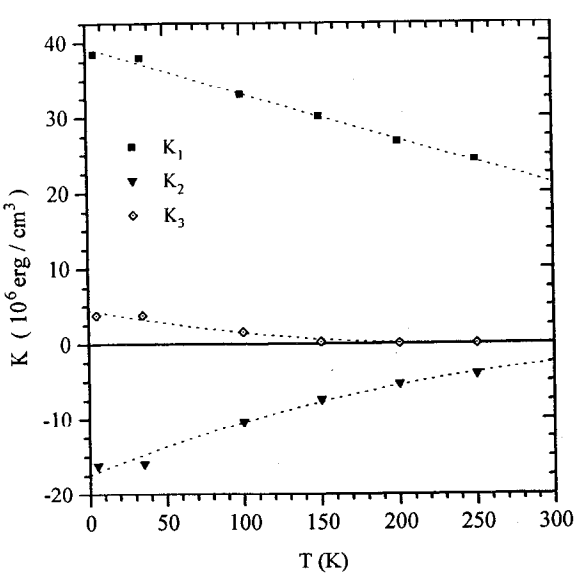

Fig. 3. Anisotropy constants K_1, K_2 and K_3 as a function of temperature for $UFe_{10}Si_2$. The lines are guides to the eye.

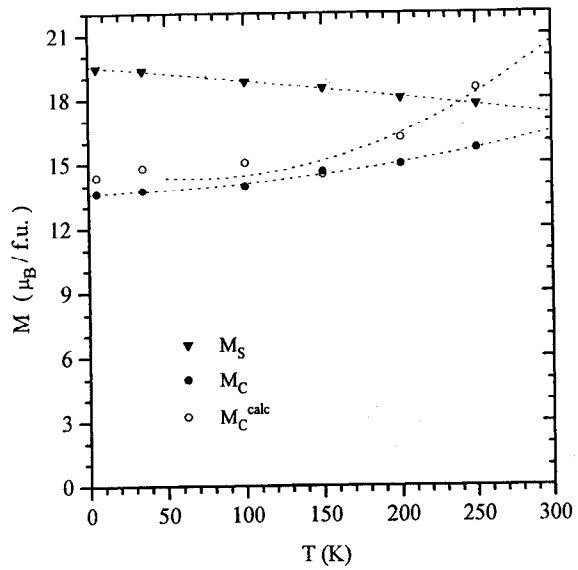

Fig. 4. Saturation magnetisation M_S, critical magnetisation M_C, and critical magnetisation calculated from the anisotropy constants M_C^{calc} (see text) for $UFe_{10}Si_2$. The lines are guides to the eye.

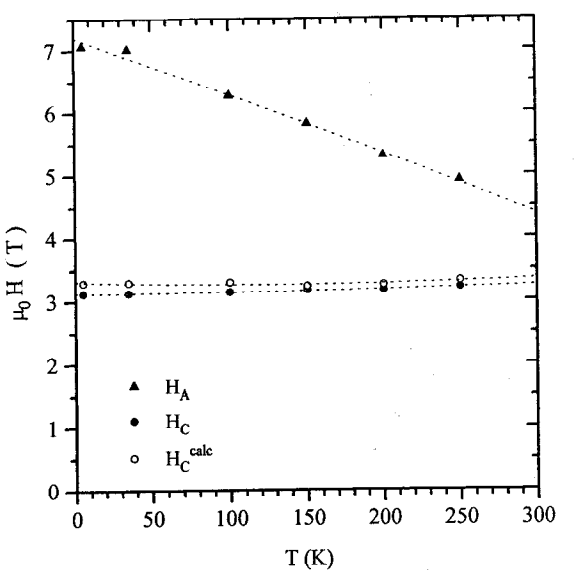

Fig. 5. Anisotropy field H_A, critical field H_C, and critical field calculated from the anisotropy constants H_C^{calc} (see text) for $UFe_{10}Si_2$. The lines are guides to the eye.

except for higher temperatures ($T \sim 250$ K) where the calculated value is higher than the saturation magnetisation. This deviation indicates that the FOMP should occur up to these temperatures. H_C^{calc} is almost constant (3.30 T at $T = 5$ K and 3.32 T at $T = 250$ K) in agreement with the experimental values: $H_C(5\ K) = 3.13$ T and $H_C(250\ K) = 3.22$ T.

Without taking into account the anisotropy constant K_3, the critical magnetisation and field values cannot be reasonably extracted from the anisotropy energy expression. For example, from the anisotropy con-

stants values obtained by Andreev et al. [9], $K_1 = 30 \times 10^6$ erg cm^{-3} and $K_2 = -9 \times 10^6$ erg cm^{-3}, a critical field $H_C(4.2\ \text{K}) = 2.7$ T is obtained instead of the 3.2 T observed value.

In systems with two magnetic sublattices, even if the individual sublattice anisotropy constants are negligible, the magnetic energy has to be described with high order effective anisotropy constants. In the present case the importance of the effective K_3 value clearly denotes a significant coupling between the iron and uranium sublattices.

Assuming a description of the 5f electrons within a localised model, the exchange interaction between the iron and uranium sublattices can be estimated from a standard mean-field analysis by comparison with the results for $YFe_{10}Si_2$ (Y is nonmagnetic). The exchange interaction between the U and Fe sublattices is given by

$$(J_{UFe}/k_B)^2 = \frac{9T_C(T_C - T_C^Y)}{4Z_{UFe}Z_{FeU}S_{Fe}(S_{Fe}+1)G_U}$$

while the Fe–Fe exchange interaction is

$$J_{FeFe}/k_B = \frac{3T_C^Y}{2Z_{FeFe}S_{Fe}(S_{Fe}+1)}$$

where Z_{AB} is the number of B neighbours to the A atom, S_{Fe} is the quasi-spin of the Fe atoms (defined by $\mu_{Fe} = 2S_{Fe}$), $G_U = (g_U - 1)^2 J(J+1)$ is the De Gennes factor and T_C^Y is the Curie temperature for the Y-compound.

For $YFe_{10}Si_2$, $T_C = 558$ K and $M_S = 18.3\ \mu_B$ f.u.$^{-1}$ [7]. From these values one obtains $\mu_{Fe} = 1.83\ \mu_B$ and $J_{FeFe}/k_B = 48.2$ K. The De Gennes factors are $G_U = 0.80$ for U^{4+} ions and $G_U = 1.84$ for U^{3+} ions. Thus J_{UFe}/k_B decreases from +44.6 K to +29.4 K when going from U^{4+} to U^{3+} ions. This interaction energy is much stronger than that obtained in the compounds with magnetic rare earths, e.g. $J_{GdFe}/k_B = -9.9$ K in $GdFe_{10}Si_2$ [20].

It should be kept in mind that, mainly due to the itinerant character of the uranium 5f electrons, this approach is not expected to be entirely correct in $UFe_{10}Si_2$, giving just an indication of the strength of the exchange interactions assuming some degree of localisation of the 5f electrons.

4. Conclusion

In conclusion, these single crystal studies allowed clear confirmation of the uniaxial magnetic anisotropy of the ferromagnetic state of $UFe_{10}Si_2$ and the occurrence of a type-1 FOMP for the hard magnetisation direction. Furthermore, the magnetic anisotropy constants were obtained and the FOMP was shown to correspond to a rotation process of the total magnetisation. The temperature independent FOMP critical field derived from the anisotropy constants is in good agreement with the experimental values. The anisotropy constants also denote a significant contribution of the U atoms to the magnetic anisotropy of the compound. The comparison with isostructural nonmagnetic rare earth compounds indicates a ferromagnetic interaction between the iron and uranium sublattices with a uranium magnetic moment of 1.4 μ_B and an important exchange interaction between the uranium and iron atoms which could be responsible for the high Curie temperature of $UFe_{10}Si_2$.

Single crystal neutron diffraction experiments, now in progress, are expected to shade some light on the magnetic structure of this compound.

Acknowledgements

This work was partially supported by JNICT (Portugal) under contract PRAXIS/3/3.1/FIS/29/94 and by NATO through Collaborative Research Grant Nr. 920996.

References

[1] W. Suski, A. Baran and T. Mydlarz, *Phys. Lett. A, 136* (1989) 89.
[2] T. Berlureau, B. Chevalier, L. Fournes and J. Etourneau, *Mater. Lett., 9* (1989) 21.
[3] P.P.J. van Engelen and K.H.J. Buschow, *J. Magn. Magn. Mater., 84* (1990) 47.
[4] M. Zelený, M. Rotter, W. Suski, A. Baran and F. Zounová, *J. Magn. Magn. Mater., 98* (1991) 25.
[5] T. Berlureau, B. Chevalier, P. Gravereau, L. Fournes and J. Etourneau, *J. Magn. Magn. Mater., 102* (1991) 166.
[6] A.V. Andreev, W. Suski and N.V. Baranov, *J. Alloys Comp., 187* (1992) 293.
[7] A.V. Andreev, F.G. Vagizov, W. Suski and H. Drulis, *J. Alloys Comp., 187* (1992) 401.
[8] A.P. Gonçalves, M. Almeida, C.T. Walker, J. Ray and J.C. Spirlet, *Mater. Lett., 19* (1994) 13.
[9] A.V. Andreev, M.I. Bartashevich, H.A. Katori and T. Goto, *J. Alloys Comp., 216* (1994) 221.
[10] A.P. Gonçalves, G. Bonfait, M. Almeida, P. Estrela, M. Godinho and J.C. Spirlet, *J. Magn. Magn. Mater., 140–144* (1995) 1419.
[11] M. Wulff, G.H. Lander, B. Lebech and A. Delapalme, *Phys. Rev. B, 39* (1989) 4719.
[12] A.C.T. North, D.C. Phillips and F.S. Mathews, *Acta Crystallogr. A, 24* (1968) 351.
[13] J.O. Lundgren, Crystallographic Computer Programs, *Rep. UUIC-B13-04-05*, 1982 (Institute of Chemistry, University of Uppsala).
[14] J.A. Ibers and W.C. Hamilton (eds.), *International Tables for X-Ray Crystallography*, Vol. 4, *Revised and Supplementary Tables*, Kynoch, Birmingham, 1974.
[15] J.P. Becker and P. Coppens, *Acta Crystallogr. A, 30* (1974) 129.
[16] J.P. Becker and P. Coppens, *Acta Crystallogr. A, 31* (1975) 417.

[17] T. Hahn (ed.), *International Tables for Crystallography*, Vol. A, *Space Group Symmetry*, Reidel, Dordrecht, 1983.
[18] K.H.J. Buschow, *J. Appl. Phys., 63* (1988) 3130.
[19] C. Lin, G.Z. Li, Z.X. Liu, H.W. Jiang, Z. Wan, J.L. Yang, B.S. Zhang and Y.F. Ding, *J. Appl. Phys., 70* (1991) 6543.
[20] Q. Li, Y. Lu, R. Zhao, O. Tegus and F. Yang, *J. Appl. Phys., 70* (1991) 6116.
[21] A.V. Andreev, Ye.V. Scherbakova, F.G. Vagizov, W. Suski, H. Drulis and T. Goto, presented at *European Magnetic Materials and Applications Conf. (EMMA '93), Kosice, Slovakis, August 24–27, 1993.*
[22] W. Suski, F.G. Vasigov, H. Drulis, J. Janczak and K. Wochowski, *J. Magn. Magn. Mater., 117* (1992) 203.
[23] Th. Sinnemann, M.U. Wisniewski, M. Rosenberg and K.H.J. Buschow, *J. Magn. Magn. Mater., 83* (1990) 259.
[24] G. Asti, in K.H.J. Buschow and E.P. Wolfarth (eds.), *Ferromagnetic Materials*, Vol.5, North-Holland, Amsterdam, 1990, p. 397.